Performance-based assessment of protection measures for buried pipes at strike-slip fault crossings

Vasileios E. Melissianos*
School of Civil Engineering – Institute of Steel Structures
National Technical University of Athens
9, Iroon Polytechneiou Str., Zografou Campus
GR-15780, Athens, Greece
email: melissia@mail.ntua.gr
tel: +302107722553

Dimitrios Vamvatsikos
School of Civil Engineering – Institute of Steel Structures
National Technical University of Athens
9, Iroon Polytechneiou Str., Zografou Campus
GR-15780, Athens, Greece
email: divamva@mail.ntua.gr
tel: +302107721935

Charis J. Gantes
School of Civil Engineering – Institute of Steel Structures
National Technical University of Athens
9, Iroon Polytechneiou Str., Zografou Campus
GR-15780, Athens, Greece
email: chgantes@central.ntua.gr
tel: +302107723440

*Corresponding author additional contact: melissianosv@gmail.com

KEYWORDS: buried pipeline, fault rupture hazard, protection measures, performance assessment

ABSTRACT

Onshore buried steel pipelines are vulnerable to fault rupture, where large ground displacements are imposed on the pipe and thus protection measures are often necessary to avoid failure. A three-step methodology based on the framework of performance-based earthquake engineering is presented on assessing the effectiveness of protection measures against the consequences of strike-slip faulting on pipes. Firstly, the probabilistic nature of the fault movement is quantified, next the pipeline mechanical behavior is numerically assessed and finally the results are combined to extract the strain hazard curves, which are easy-to-handle engineering decision making tools. The various protection methods used in engineering practice or proposed in the literature are evaluated through the mean annual rate of exceeding strain values, also including a simple safety checking format at the strain level. Conclusions are extracted from the proposed assessment methodology on the efficiency of measures with reference to engineering practice and safety requirements of the pipeline operator.

1. INTRODUCTION

Onshore buried steel pipelines are the main means of fossil fuel transportation and are critical lifelines for both the society and the global economy. However, pipelines located in seismic areas shall inevitably cross tectonic seismic faults, whose activation results to imposed large permanent ground displacements on the crossing pipeline. In major past earthquake events, fault movement has been found to be the dominant cause of pipeline failure compared to other seismic-induced actions, such as wave propagation [1]. The principal failure modes in such case are local buckling of the pipe wall due to developing compression and tensile fracture of girth welds between adjacent pipeline parts due to concentration of tensile strains. Taking into account that any potential pipeline failure may result to environmental pollution, economic losses and directly or indirectly to human injuries, it is deemed appropriate to establish a methodology for seismic risk assessment and to introduce protection measures to avoid the aforementioned repercussions.

Earthquakes are typical phenomena that are characterized by high randomness. This fact raises the question as to the appropriate magnitude of fault offset that has to be taken into account in the earthquake resistant design of buried pipes. In the commonly applied deterministic approach, a single fault displacement is considered as the worst case scenario, consisting of a postulated occurrence of an earthquake with a specific magnitude at a specific location. This approach provides only a point estimate of unknown likelihood, while the effects of uncertainties encountered in the various design stages are typically neglected, or at best handled with unknown conservatism. Instead, in the probabilistic approach it is attempted to quantify the probabilistic nature of the loading, given that the available knowledge and understanding of fault movement is inadequate. This approach allows the design of a new or the assessment of an existing pipeline at a pre-defined level of risk that is consistent with a desired allowable lifetime probability, as mandated by financial, regulatory and legal constraints. Therefore, a better balance between economy, safety and environmental responsibility can be accomplished. This probabilistic approach is thus adopted here.

The proposed methodology for seismic risk assessment of buried pipelines at fault crossings consists of three interrelated steps: (1) conduct seismic hazard analysis to quantify the fault displacement hazard, (2) perform pipeline structural analysis to obtain developing strains and then (3) combine the results to estimate the risk. The resulting risk is then used to directly compare the performance of a pipeline at a given site and thereby evaluate the effectiveness of alternative mitigating measures against the consequences of faulting. The theoretical background for the general case of unprotected buried pipelines is presented in [2]. The methodology is based on the framework for Performance-Based Earthquake Engineering of Cornell and Krawinkler [3], which has been adopted by the Pacific Earthquake Engineering Research (PEER) Center.

The appropriate tool for the seismic hazard analysis is the Probabilistic Fault Displacement Hazard Analysis (PFDHA), whose basis was introduced by Youngs et al. [4]. PFDHA aims at quantifying the mean annual rate (MAR) of exceeding (λ) various fault displacement levels at a given site. The MAR of exceedance is the primary means of representing time-related risk. Engineers are typically more familiar with the equivalent probability of exceedance over a given time period, such as the p = 10% probability of exceedance in T = 50 years being a design target for most buildings. This corresponds to a MAR of exceedance of $\lambda = -\ln(1 - p)/T = 0.0021$. In PFDHA the MAR of exceeding a fault displacement can be assessed by incorporating any available geological and seismological data, for example, fault slip rate, rupture location, fault activation probability and distribution of earthquake magnitudes along with the corresponding uncertainties. Within the present study, the aim is to extend this estimation to arrive at the MAR of exceeding given levels of pipeline strain due to faulting. The second step consists of the pipeline's structural analysis, where the maximum compressive and tensile strains are obtained, considering fault offset magnitudes obtained from the seismic hazard analysis. Finally, in the third step, results from the previous steps are combined to estimate strain hazard curves, i.e. curves of MAR of exceeding given strain levels. The evaluation of seismic risk for a selected limiting strain

value, in terms of estimating its mean annual rate of exceedance [5], is adopted in this third step to assess the pipeline seismic risk.

In case of an earthquake event, the response of buried pipes differs from other structures, such as buildings and bridges, where the foundation is forced to follow the ground movement and the superstructure is excited due to its inertia. Contrary, buried pipes are surrounded by soil and in case of fault movement, the structure is forced to follow the ground movement by developing excessive deformation and consequently significantly high strains. Therefore, the design against faulting is carried out in strain terms (Strain Based Design), rather than stress terms, as recommended by pertinent codes, for example, in ALA guidelines [6], given that the problem is displacement-controlled. The safety checking is thus expressed as:

$$\varepsilon_{dem} \leq \varepsilon_{cap} \quad (1)$$

where the strain demand $\boldsymbol{\varepsilon_{dem}}$ is obtained from the structural analysis and the strain capacity $\boldsymbol{\varepsilon_{cap}}$ is provided by structural codes and standards, where strains are limited to avoid local bucking and/or tensile fracture.

Pipe protection through minimizing the developing strains remains a top research objective both for the academia and the industry. An extensive overview, followed by a comprehensive evaluation of various seismic protection measures for buried pipes under faulting has been presented in [7]. Protection measures can be divided into three main categories:

- Friction reduction measures, which aim at reducing the pipe – soil friction that is developed on the pipe – soil interface due to the pipe movement in the trench.
- Pipe strengthening measures, which aim at increasing the pipe strength and stiffness.
- Other measures, which cannot be classified in the two previous categories.

A performance-based assessment of various mitigating measures is offered here. Initially, the seismic risk assessment theoretical background is outlined. Then, the effectiveness of measures is assessed through a case study. Special attention is paid to (1)

the demonstration of the difference between the deterministic and the probabilistic approach on assessing the efficiency of protection measures and (2) in providing a framework for pipeline operators to decide whether any proposed measure can satisfy their requirements.

2. METHODOLOGY FOR PERFORMANCE-BASED ASSESSMENT

2.1. Seismic hazard analysis

2.1.1. Fault displacement hazard

The “earthquake approach” of PFDHA that is directly derived from Probabilistic Seismic Hazard Analysis [8] is adopted, relating the occurrence of fault displacement (Δ) at a site to the occurrence of earthquakes at the fault. Only principal faulting is evaluated, without considering the contribution of distributing faulting on seismic hazard [4]. Moreover, the focus is only on-fault displacements, as the problem under investigation is a main transmission pipeline crossing a primary fault and off-fault displacements [9] are not considered.

In the application of PFDHA four factors are considered: (1) earthquake magnitude (M), (2) surface rupture length (SRL), (3) rupture position along the fault trace and (4) position of the crossing site. The earthquake magnitude stands as the key factor for describing a seismic source and ranges from a minimum value (M_{min}) of engineering significance, assuming that lower magnitudes do not contribute to the seismic hazard, to a maximum value (M_{max}), which is constrained by the fault characteristics. The range of magnitude values is discretized into a number of bins to account for all possible values. Thereafter, accepting that different earthquakes may rupture fault lengths of different size, the surface rupture length (SRL) along the fault trace is introduced as the second factor. The position of SRL on the fault trace (third element) and whether it will intercept the pipe (fourth element) are considered, admitting that earthquakes of the same magnitude may rupture fault segments of different length. Thus, it is necessary to deal with a variety of potential SRLs, each at a different position. However, due to the lack of detailed fault-specific data, it is assumed that SRLs of the same size are equiprobable. For simplicity of bookkeeping, a minimum SRL size is determined, for example, as corresponding to the minimum earthquake

magnitude of interest via empirical equations [10], while all subsequent larger SRLs are regarded as integer multiples. In practice, every SRL size is accounted for at all possible positions, keeping track of those that intercept the pipeline and thus contribute to fault displacement hazard at the pipeline crossing site.

PFDHA is implemented herein using the total probability theorem in order to estimate the MAR of exceeding fault displacement at the pipeline crossing site, denoted by $\lambda_\Delta(\delta)$. It is noted that, in general, the parameters are denoted by capital letters, for example fault displacement parameter Δ, and their discrete values by lowercase letters, for example corresponding fault displacement value δ. The MAR of exceedance is a summation over all possible distinct scenarios that could produce an exceedance of fault displacement δ:

$$\lambda_\Delta(\delta) = v \sum_i P(\Delta > \delta | m_i) P_M(m_i) \quad (2)$$

where v is the rate of all earthquakes with $M > M_{\min}$ and $P_M(m_i)$ is the probability of earthquake magnitude M, for example, according to the Gutenberg-Richter Bounded Recurrence Law [11]. Kramer [12] provides also an interesting overview on the estimation of earthquake occurrence probability. The function $P(\Delta > \delta | m_i)$ estimates the probability that fault displacement exceeds a defined value δ, given an earthquake of magnitude m_i has occurred:

$$P(\Delta > \delta | m_i) = \sum_j \sum_t \sum_k P\left(\Delta > \delta | SRL_j, FD_t, Pos_{k,j}\right) \times P\left(SRL_j, FD_t | m_i\right) \times 1/N_j \quad (3)$$

Discretization of parameters is introduced in Eq. (3) to account for all possible cases: (1) earthquake magnitude (m_i) discretization in i bins, (2) rupture length (SRL_j) discretization in j bins, (3) k = 1,2,…,N_j number of positions of the rupture length and (4) keeping track and discretization of the average or the maximum displacement of the entire fault FD_t. It is noted that FD_t characterizes the entire fault rupture regardless of location, while Δ refers to the crossing site specifically. The first right-side term of Eq. (3) is the conditional probability of exceedance $P(\Delta > \delta | SRL_j, FD_t, Pos_{k,j})$, which is the core of PFDHA and requires detailed calculations that are carried out over each combination of bins of earthquake magnitude, rupture length, fault displacement and all possible positions of SRL_j along the fault trace. The

second right-side term of Eq. (3) is the joint probability of *SRL* and *FD*, conditional on the earthquake magnitude. Wells and Coppersmith [10] provide empirical expressions to calculate this probability by correlating SRL with the average fault displacement (AD) or the maximum fault displacement (MD). AD and MD fault displacement are alternative approaches of PFDHA for the estimation of FD and are used to normalize fault displacement data sets throughout calculation of the fault displacement prediction equation. It is essential to highlight the fact that the usual design approach is deterministic, as design engineers use the mean values from empirical (regression) relationships of fault characteristics, for example, obtained from [10], and neglect their dispersion. The proposed methodology incorporates both the dispersion and the correlation among fault characteristics in order to quantify the randomness of fault offset magnitude.

2.1.2. Fault movement

Focus in standard PFDHA methodology is on the magnitude of fault offset, while the distribution into x/y/z spatial components is often neglected. Nevertheless, fault movement is three-dimensional in nature. The distribution of fault displacement components provides the fault type characterization as normal, reverse or strike-slip and consequently determines the pipeline structural response. Past earthquake events have demonstrated that strike-slip faulting causes pipeline bending and tension/compression, normal faulting causes pipeline bending and tension, while reverse faulting causes pipeline bending and compression. More details regarding the general approach for faults having multiple non-zero displacement components can be found in [2]. Here, for illustration purposes only the conceptually simpler pure strike-slip case is considered, targeting the same general problem as tackled by Cheng and Akkar [13] via a Monte Carlo approach.

The general case of the geometry of a pipeline – fault crossing is depicted in plan view in Figure 1, where Δ_1 is the fault-trace-parallel horizontal component and Δ_2 is the fault-trace-normal horizontal component. It is noted that for strike-slip fault type it states that $\Delta_2 = 0$, while for normal or reverse fault type it is $\Delta_2 > 0$, where Δ_2 is obtained from the fault vertical movement and the fault dip angle. The considered pipeline segment is assumed to

be straight, as dictated by good engineering practice and code provisions in the vicinity of faults, as any bends may lead to the introduction of undesirable additional forces due to route change. The fault is assumed to be planar without thickness, thus appearing on the ground surface as a straight line that is referred as the fault trace. Then, the global coordinate system (1,2) refers to the fault movement, while (x,y) is the local coordinate system of the pipe. The imposed displacements on the pipeline, namely in the longitudinal and transverse directions with respect to the pipeline axis, Δ_x, and Δ_y, respectively, are obtained through the rotation of the global coordinate system by the pipeline – fault crossing angle β. For strike-slip fault type in particular, fault component Δ_1 equals the fault displacement Δ and thus regarding the MAR of exceedance it is obtained:

$$\lambda_{\Delta}(\delta) = \lambda_{\Delta_1}(\delta_1) \tag{4}$$

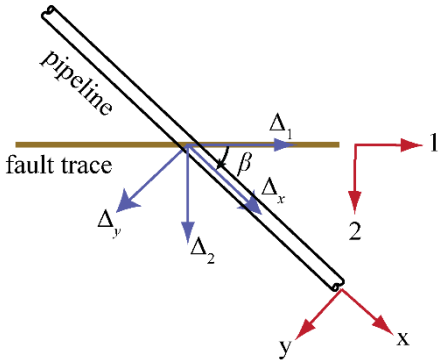

Figure 1: Pipeline – fault crossing geometry in plan view (adapted from [2])

2.1.3. Seismic hazard uncertainty

The randomness of the earthquake loading necessitates the consideration of pertinent uncertainties through the seismic hazard analysis, otherwise results could become sensitive to extreme scenarios or in other words to the specific parameters adopted [14]. Any quantifiable uncertainty can be incorporated in PFDHA. Epistemic uncertainties are related to the inadequate knowledge of seismological parameters and can be in time reduced with better observations. These uncertainties, in practice, lead to multiple alternative hazard curves and are handled through logic trees, considered to be the state-of-the-art tool for quantifying and incorporating epistemic uncertainties in the seismic hazard calculation. A weight factor is assigned in every tree branch, representing the engineer's degree of belief in

the alternative models [15]. Thus, every alternative scenario has a total weight factor, which is the product of the associated partial weight factors.

The three-level logic tree of Figure 2 is adopted here, including the seismic rate v, the maximum earthquake magnitude M_{max} and the fault displacement estimation approach of PFDHA. Seismic rate is defined as the rate of exceeding M_{min} and is the dominant feature of the seismic source, while being subjected to high uncertainty, as its mean value is an estimate provided by seismologists. Maximum magnitude is another seismological parameter under question. The minimum magnitude, in contrast, is only a limiting factor to define the events that are of engineering interest and its value does not influence the estimates, thus not appearing in Figure 2. Finally, using either the average or the maximum fault displacement within PFDHA constitutes two modeling options that yield slightly different results and are thus incorporated as uncertain parameters. In practice, each branch of v alternatives is weighted by wv_i and further broken to branches of M_{max} (weighted by wM_i), themselves splitting into the AD versus MD option of PFDHA (weighted by wD_i). Finally, it is noted that aleatory uncertainties are incorporated by employing and appropriately sampling the distributions for the probabilistic quantities appearing in Eq. (3), as described in section 2.1.1.

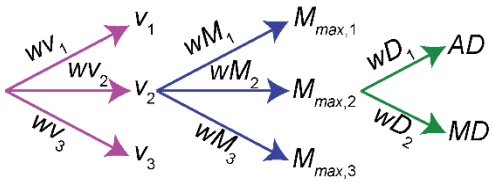

Figure 2: The three-level logic tree adopted for seismic hazard uncertainty analysis (adapted from [2])

2.2. Pipeline structural analysis

The pipeline structural analysis is an integral part of buried pipeline – fault crossing seismic risk assessment, providing the pipeline response due to the imposed ground displacements, or in other words the conditional pipeline demand. Within the proposed methodology the engineer is asked to perform structural analyses for fault displacement (Δ)

ranging from a sufficiently small value that does not cause pipeline failure, to a larger one that shall definitely lead to failure. The output of the structural analysis consists of the maximum tensile and compressive strain demands. The locations where the maximum strains develop are not considered, assuming that the same section will not fail due to compression and tension simultaneously.

Buried pipeline response under faulting is dictated by the pipe – soil interaction and soil nonlinear behavior. Thus, the implementation of advanced numerical analysis techniques is indispensable in the design and analysis of buried pipes to withstand large fault offsets. There are two pertinent modeling approaches: (1) the beam-type FEM model, where the pipeline is meshed into beam-type finite elements and the surrounding soil is modeled with translational springs, for example [16]-[18], and (2) the continuum model, where the pipeline is meshed into shell finite elements and the surrounding soil into 3D-solid elements. The continuum model is considered to be rigorous, as among other parameters local buckling of the pipe can be assessed, more advanced soil material laws can be adopted and trench boundaries can be incorporated in the analysis, for example [19]-[21]. Yet, the continuum model overly increases the complexity of the problem, the required computational power and moreover convergence problems can emerge in the interface of pipe – soil. Its applicability is thus quite limited in engineering practice.

A beam-type FE model is formulated in the present study taking advantage of its generally acceptable balance between accuracy, reliability and reduced computational effort. The model is based on the suggestions of Eurocode 8 – Part 4 [22] and ALA guidelines [6] and provides the ability to capture, directly or indirectly, the main effects and pipe failure mechanisms. Hence, the pipeline is modeled with beam finite elements that can describe the bending and axial deformation of the pipe and also provide stresses and strains at predefined locations, namely the integration points on cross-sections along the pipeline. Soil is represented by a series of mutually independent nonlinear translational springs, based on the Winkler model (Figure 3) in the axial, transverse horizontal, vertical upward and vertical downward direction. The differential ground movement is applied statically on the pipeline as

imposed displacements on the corresponding “ground nodes” of spring elements on the fault hanging wall, while the “ground nodes” on the fault footwall are fixed. This modeling approach is based on the assumption that the planar fault divides the earth crust into two soil blocks, for example [16],[21].

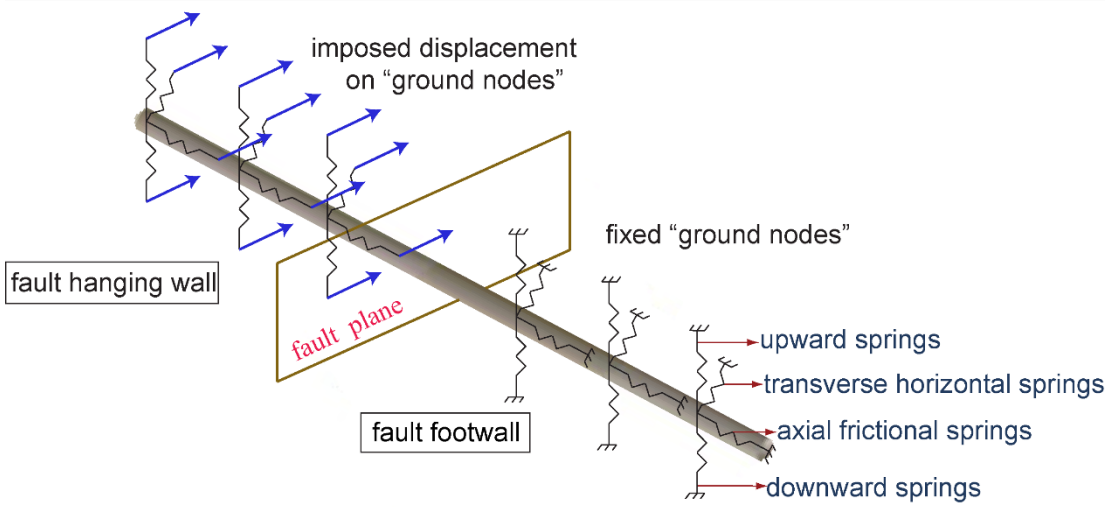

Figure 3: Pipeline – fault crossing beam-type FE model (adapted from [7])

2.3. Pipeline strain hazard analysis

In seismic hazard analysis, the interaction between the seismologist and the structural engineer is achieved by means of an interface variable that is also known as the intensity measure (IM). For a building, the IM could be for example the peak ground acceleration, but the proper IM quantity for the problem under investigation is the magnitude of the fault offset and in particular for a strike-slip fault it is a single scalar. It should be noted that if the proposed methodology is extended to encompass failure mechanisms related to the cyclic nature of loads, for example fatigue, rather than their peak value, then the adopted IM might not be sufficient.

The development of strain hazard curves, which are the engineering output of the proposed methodology, necessitates the calculation of the MAR of exceedance of strains. The engineer is thus asked to select a range of tensile and compressive strain values that should comprise the demand values. Strain values are then sufficiently discretized into a number of bins and the strain hazard curve is calculated by summing the MAR of equaling

tensile (ε_t) and compressive (ε_c) strains. So, the mean annual rate of equaling $\Delta\lambda_\varepsilon(\varepsilon_c,\varepsilon_t)$ for strains that fall within each bin is estimated via the expression:

$$\Delta\lambda_\varepsilon(\varepsilon_c,\varepsilon_t) = \sum_{\substack{\varepsilon_{c,ij}\epsilon I[\varepsilon_c] \\ \varepsilon_{t,ij}\epsilon I[\varepsilon_t]}} \Delta\lambda_\Delta(\delta_i) \quad (5)$$

where $\varepsilon_{c,ij}$ and $\varepsilon_{t,ij}$ are the strain estimates (demand) for concurrent fault displacement components δ_i and $I[\varepsilon] = [\varepsilon - \alpha, \varepsilon + \alpha]$, where 2α is the bin width for discretizing strains. In order to perform this task, it is efficient to perform pipeline structural analysis for a range of fault displacement values Δ that convey the entire range of pipeline response, i.e. from no damage to failure. Moreover, $\Delta\lambda_\Delta(\delta)$ is the MAR of equaling of fault displacement. The bins of MAR of exceedance λ_Δ are changed to the bins of MAR of equaling through appropriate discretization:

$$\Delta\lambda_\Delta(\delta) = |\lambda_\Delta(\delta + w) - \lambda_\Delta(\delta - w)| \quad (6)$$

where $2w$ ($w > 0$) is the displacement bin width and by definition $\Delta\lambda_\Delta(\delta) > 0$.

The strain hazard estimation provides the MAR of equaling of strains and consequently, the strain hazard curves are derived by their selective summation. The estimation of the MAR of exceeding strain limit states is crucial within the framework of seismic risk assessment. Two failure limit states are introduced: (1) local buckling and (2) tensile fracture. In general, any limit state can be introduced in the process to also evaluate lesser consequences, for example, pipeline damage without leakage.

The MAR of exceeding tensile ($\lambda_{\mathrm{LS},t}$) and compressive ($\lambda_{\mathrm{LS},c}$) strain limit states, respectively, is estimated for the strike-slip faulting case (see [2] for the general case) via the expressions:

$$\lambda_{\mathrm{LS},t} = \sum_{\varepsilon_c,\varepsilon_t} P\left(\varepsilon_{dem} > \varepsilon_{t,cap}\right) \Delta\lambda_\varepsilon(\varepsilon_c,\varepsilon_t) \quad (7)$$

$$\lambda_{\mathrm{LS},c} = \sum_{\varepsilon_c,\varepsilon_t} P\left(\varepsilon_{dem} > \varepsilon_{c,cap}\right) \Delta\lambda_\varepsilon(\varepsilon_c,\varepsilon_t) \quad (8)$$

where $\Delta\lambda_\varepsilon(\varepsilon_c,\varepsilon_t)$ is the MAR of equaling of strains after Eq. (5). $P(\varepsilon_{dem} > \varepsilon_{cap})$ is the fragility function of strain demand exceeding strain capacity, which becomes a step function of the strain demand, assuming demand and capacity are non-random:

$$P\left(\varepsilon_{dem} > \varepsilon_{cap}\right) = \begin{cases} 0, \varepsilon_{dem} < \varepsilon_{cap} \\ 1, \varepsilon_{dem} > \varepsilon_{cap} \end{cases} \quad (9)$$

If the strain results of structural analysis are formalized as deterministic function of fault displacement Δ, i.e. $\varepsilon_t = h(\Delta)$ and $\varepsilon_c = h(\Delta)$, then Eqs (7) and (8) are simplified, respectively, to:

$$\lambda_{\mathrm{LS},t} = \lambda_{\Delta}\left(h^{-1}\left(\varepsilon_{t,cap}\right)\right) \quad (10)$$

$$\lambda_{\mathrm{LS},c} = \lambda_{\Delta}\left(h^{-1}\left(\varepsilon_{c,cap}\right)\right) \quad (11)$$

2.4. Safety factor format

Demand and capacity are inherent random quantities. Material variability, manufacturing tolerances, welding quality etc. may introduce additional uncertainty in the demand and capacity of the pipeline. Their influence will probably be significant for aged and not well-maintained pipes [23]. On the other hand, newer and well-constructed pipes will be subject to considerably less uncertainties, whose importance will tend to be overshadowed by the uncertainty in the seismic hazard. At the same time, the uncertainty in the hazard itself is also significant.

A typical Load and Resistance Factor Design (LRFD) format for checking capacity ε_{cap} against demand ε_{dem} involves the two corresponding partial safety factors γ_{cap} and γ_{dem} as follows:

$$\frac{\varepsilon_{cap}}{\gamma_{cap}} > \varepsilon_{dem}\gamma_{dem} \Rightarrow \frac{\varepsilon_{cap}}{\varepsilon_{dem}} > \gamma_{cap}\gamma_{dem} \quad (12)$$

The two factors depend on the distribution of ε_{cap} and ε_{dem}, herein assumed to be lognormal with dispersions β_{uC} and β_{uD}, respectively. If *CDR* is defined as the capacity-to-demand ratio and $SM = \gamma_{cap}\gamma_{dem}$ as the required safety margin, in order to achieve an x% confidence of no failure with 50% ≤ x < 90%, one can exploit the lognormality of *CDR* to require [5]:

$$CDR > SM \Rightarrow \frac{\varepsilon_{cap}}{\varepsilon_{dem}} > \exp(k_x\beta_u) \quad (13)$$

where $k_x = \Phi^{-1}(1\text{-}x)$ is the normal variate corresponding to a confidence level of x% and $\Phi^{-1}(\cdot)$ is the inverse standard normal cumulative distribution function. Moreover, β_u is the

overall uncertainty in capacity and demand that, assuming independence of ε_{cap}, ε_{dem}, is estimated as:

$$\beta_u = \sqrt{\beta_{uC}^2 + \beta_{uD}^2} \tag{14}$$

In simpler words, the capacity-to-demand ratio (*CDR*) needs to be higher than the appropriate safety margin (*SM*) that is commensurate with the overall uncertainty in the problem.

The deterministic (unfactored) assessment case corresponds to x = 50% and SM = 1, whereby there is a 50% probability that the pipe will exceed the limit state, which is the case of having an equality in Eq. (12) is achieved. In general, a 95% confidence is practically standard requirement of modern guidelines, for example in FEMA 350 [24] and EN 1990 [25], while the dispersions β_{uC} and β_{uD} themselves are a matter of the magnitude of uncertainty in capacity and demand. A minimum value for both might be $\beta_{uC} = \beta_{uD} = 0.25$, assuming excellent knowledge of the pipeline response and material fracture properties, while higher values of 0.30 to 0.40 are a more reasonable representation of practical applications.

It is finally noted that the incorporation of demand and capacity uncertainties is presented here in a simplified way for practical design and assessment purposes, while more details on incorporating these uncertainties in a more comprehensive performance assessment can be found in [2].

3. PROTECTION MEASURES

Design of pipes is carried out within a strict framework of laws and regulations considering that pipe failure is practically unacceptable. However, pipelines extend over long distances and fault crossings cannot be always avoided when seismic areas are traversed, even though this is suggested by pertinent codes, for example in ALA [6] and Eurocode 8 – Part 4 [22]. Therefore, various protection measures are applied in practice and others have been examined by researchers in order to minimize the potential of pipe failure. The following measures are evaluated here on a performance basis:

- Trench backfilling with pumice (case P) that aims at reducing friction [26].
- Pipe placing within prefabricated concrete culverts (case C) without backfill soil that aims at “eliminating” friction.
- Introducing hinged bellow-type flexible joints (PFJ) in the pipe in the fault vicinity that aims at concentrating strains at the joints and retaining pipe steel unstressed by transforming the pipe structural system from continuous to segmented. This measure has not been applied yet in practice, but results presented in [27] and [28] indicate that it is a promising solution.
- Steel grade upgrading (case S) and pipe wall thickness increasing (W) that aim at improving pipe strength and/or stiffness [26],[29].

All protection measures are applied along the pipe at a distance that is defined by the fault trace uncertainty, namely the distance over which the fault trace might appear on or very close to the ground surface.

An additional comment is that even though pipe protection in fault crossings remains a “hot” topic for researchers, designers, pipe operators and regulatory authorities, pertinent research efforts are quite limited, compared to those that deal with the assessment of pipe structural behavior. The present study aims at contributing towards filling this research gap by evaluating the efficiency of measures on a performance basis, adopting the state-of-art tools of earthquake engineering [30].

4. CASE STUDY

4.1. Pipeline – fault crossing

A typical API5L-X65 transmission pipeline is considered (reference pipeline, abbreviated as R), featuring a cross-section with external diameter 914mm (36in) and thickness 12.7mm (0.5in). The steel properties are: nominal yield stress 448.5MPa and ultimate stress 531MPa, elastic modulus 210GPa, Poison ratio 0.3 and ultimate strain 18%. The pipeline is assumed to be corrosion- and defect-free and coated with coal-tar. The pipe is embedded under 1.3m of cohesionless loose sand with unit weight 18kN/m^3 and internal

friction angle 36^o. The tensile and compressive strain limits, which are the strain capacity terms, after ALA – Appendix B [6] for the pipeline under investigation are $\varepsilon_{t,cap}$ = 2% and $\varepsilon_{c,cap}$ = 0.39%, respectively, corresponding to operable conditions.

A strike-slip fault is considered with fault trace length equal to 40km. The pipeline crossing is located at distance equal to 10km from the fault closest edge. Pipe – fault crossing angles equal to β = 75^o and β = 90^o (Figure 1) are considered, which represent indicative values that lead to pipe bending and elongation (β = 75^o) and pipe predominant bending (β = 90^o). The fault is assumed to intercept the pipe at the middle of its modeled length. The seismological and uncertainty parameters considered in the case study are listed in Table 1 and have been selected here only for illustrative reasons. In each specific case at hand one should use appropriate weight factors and seismological parameters, for example for European faults one could adopt values from the EU-SHARE seismological models [31],[32]. The minimum earthquake magnitude under consideration is $M_{\min}$ = 4.50. The minimum and maximum fault displacement values taken into account in seismic hazard analysis can be estimated using the empirical expression of Wells and Coppersmith [10], where the average fault displacement (AD) is related with earthquake magnitude:

$$\log\left(\widehat{\Delta}_{\text{average}}\right) = -6.32 + 0.90M \quad (15)$$

where $\widehat{\Delta}_{\text{average}}$ is the median estimate of the average fault displacement. The AD approach is employed, rather than the MD, based on the suggestions of Wells and Coppersmith [10] regarding the maximum fault offset occurrence at fault crossings. Considering the minimum magnitude $M_{\min}$ = 4.5 and the maximum $M_{\max}$ = 7.3, Eq. (15) yields a median (50%) estimate of $\widehat{\Delta}_{\text{average}}$ from 0.005m to 1.78m. At the higher end, the 84% estimate can be used to offer a wider and more reasonable range of probable fault offset values, leading roughly to 3.40m. At the lower end, a value of 0.01m is employed instead of 0.005m as having more engineering significance for an operable limit-state.

Table 1: Seismological data and corresponding uncertainty weight factors considered in the case study.

parameter	weight factor	parameter	weight factor	parameter	weight factor
$v_1 = 1.20$	$wv_1 = 0.30$	$M_{max,1} = 7.1$	$wM_1 = 0.25$	AD	$wD_1 = 0.50$
$v_2 = 1.40$	$wv_2 = 0.40$	$M_{max,2} = 7.2$	$wM_2 = 0.50$	MD	$wD_2 = 0.50$
$v_3 = 1.60$	$wv_3 = 0.30$	$M_{max,3} = 7.3$	$wM_3 = 0.25$		

4.2. Numerical modeling

A beam-type FE model (Figure 3) is developed for the analysis of the pipe – fault crossing, using the general purpose commercial FEM software ADINA [33]. The pipeline is meshed into 4000 PIPE elements that are two-node Hermitian beam elements with element length equal to 0.25m, following a mesh density sensitivity analysis. The surrounding soil is represented by nonlinear translational SPRING elements, which connect “ground nodes” to corresponding pipe nodes and exhibit stiffness only along the local longitudinal axis. Spring properties are estimated according to ALA guidelines [6], assuming that the backfill properties are similar to those of the native soil.

Numerical analyses are performed by taking into account the numerical considerations presented in [34] and the suggestions in [35], using the Newton-Raphson solution algorithm. Fault movement is treated as a quasi-static phenomenon and consistency with this fact is achieved by selecting an appropriate number of solution steps in order to (1) achieve numerical convergence and (2) allow the imposed displacement (fault offset) to be applied smoothly. As an additional remark, non-seismic and operational loads, for example, internal pressure, external earth pressure, etc., are not considered.

4.3. Protection measures

The protection measures presented in section 3 are applied along the total fault trace uncertainty length, which is assumed to be 100m on each side of the fault trace. Details on the numerical modeling of every measure are as follows:

- The trench is backfilled with pumice (case P) having unit weight 8kN/m^3, cohesion 0kPa and internal friction angle 33^o. The soil spring properties are estimated according to ALA guidelines [6] and in particular axial, transverse horizontal and vertical upward springs are modified vis-a-vis the reference pipe, while vertical downward springs are not, as the spring constants are calculated using the native soil properties.
- The pipe is placed within concrete culverts (case C) and modeled by removing the soil springs along the length of the pipe, where culverts are installed without backfill soil between the pipe and the culvert.
- Hinged bellow-type flexible joints are introduced in the pipe (PFJ) following the preliminary design guidelines presented in [27]. Joints are modeled as generic flexible joints, represented by a rotational spring at the center point without modeling the joint length [36], while the joint's lateral and axial relative movements of the two ends are restrained. Joint torsional movement is also restricted through appropriate constraints as rotation about the longitudinal axis is generally prohibited by the manufacturers [37]. Flexible joints introduced in the pipeline exhibit rotational stiffness equal to 100kN/rad.
- The steel grade is upgraded (case S) to API5L-X80 having elastic modulus 210GPa, yield stress 530MPa, yield strain 0.25%, failure stress 621MPa and failure strain 18%. Numerical modeling is carried out by modifying the steel properties of the reference pipe (R) along the uncertainty length.
- The pipe wall thickness is increased (W) from 12.70mm to 19.05mm, both being commercially available thickness values. Numerical modeling is performed by increasing the pipe wall thickness of the reference pipe (R) along the uncertainty length.

The examined measures are summarized in Table 2, providing an overview of the case study. Finally, it is assumed that in all cases the trench is wide enough for the boundaries not to affect the properties of transverse horizontal springs.

Table 2: Protection measures under investigation in the case study.

Case	Protection measure	Measure type	Steel grade	Wall thickness	Backfill soil
R	(reference pipe)	–	X65	12.70mm	sand
P	Trench backfilling with pumice	group 1	X65	12.70mm	pumice
C	Use of culverts	group 1	X65	12.70mm	–
PFJ	Use of flexible joints	group 1	X65	12.70mm	sand
S	Steel grade upgrade	group 2	X80	12.70mm	sand
W	Wall thickness increase	group 2	X65	19.20mm	sand

5. PRESENTATION AND DISCUSSION OF RESULTS

The proposed methodology for performance assessment of protection measure for buried pipes at fault crossings consists of three steps. In order to provide deeper comprehension of the proposed methodology, indicative results for the reference pipe (R) from every step are presented in Figure 4, considering the pipe – fault crossing angle β = 90°. Firstly, the seismic hazard analysis (section 2.1) is carried out for each of the 18 scenarios listed in Table 1 according to the logic tree of Figure 2 by applying Eqs. (2) and (3). Thus, 18 hazard curves are produced, which are combined through the logic tree of Figure 2 to produce the mean fault displacement hazard curve at the pipe crossing site. The descending curve shape is predictable, as the higher the fault displacement Δ is, the lower the MAR of exceedance λ_Δ becomes. It is noted that seismic hazard analysis is independent of the pipeline structural system.

Secondly, the pipeline structural analysis is carried out (sections 2.2 and 4.2). Structural analysis results are presented in terms of the maximum tensile and compressive strain with respect to the fault offset Δ normalized by the pipe diameter D (Δ/D). It has to be noted that when a pipe is subjected to bending and tension due to faulting, which is the case for pipe – fault crossing angle $\beta \leq 90^o$, then the strain-state depends on the fault offset magnitude. Strain results presented in this study are the longitudinal tensile normal strains that are the summation of axial and bending strains. For low fault offset the pipe behavior is

dominated by bending. As fault offset increases further predominant tension develops in the pipe. Between these two strain-states, there is a transition from flexural to axial behavior that explains the low strain rate increase (roughly from 1.5Δ/D up to 3.0Δ/D). Then, as stated before, the pipe is severely elongated and consequently there is a sharp strain increase. This effect has been explained by the authors in detail in [7] and [27]. Any sharp bends in the tensile strain distributions of the following figures are attributed to this evolution of the pipe strain-state with respect to fault offset increase.

The third step is the pipe strain hazard analysis (section 2.3), where results are presented by means of the strain hazard curves, where the MAR of exceeding strain values is presented on the vertical axis and the corresponding strains on the horizontal axis. Additionally, the vertical line represents the code-based strain limit after ALA [6]. The horizontal line stands for the 10% probability of failure in 50 years, or failure with return period 475 years, or equivalently a MAR of exceedance equal to $\lambda = 21\times10^{-4}$. Moreover, the MAR of exceeding a strain limit state is obtained through Eqs. (10) and (11), or by the intersection of the strain hazard curve and the code-based strain limit line.

Methodology step	Analysis	Result
1st	Seismic hazard analysis	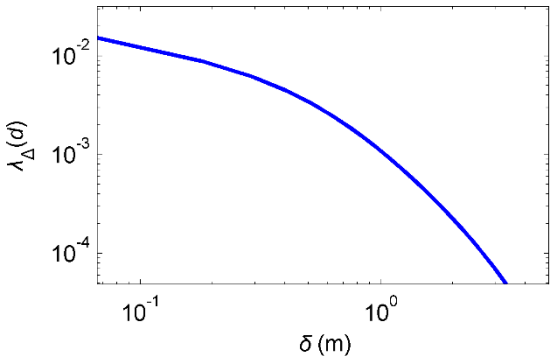
2nd	Pipeline structural analysis	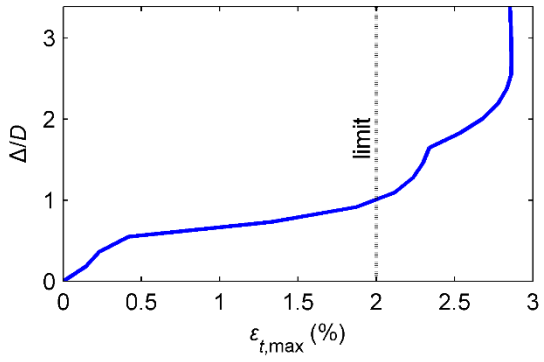

3rd	Pipeline strain hazard analysis	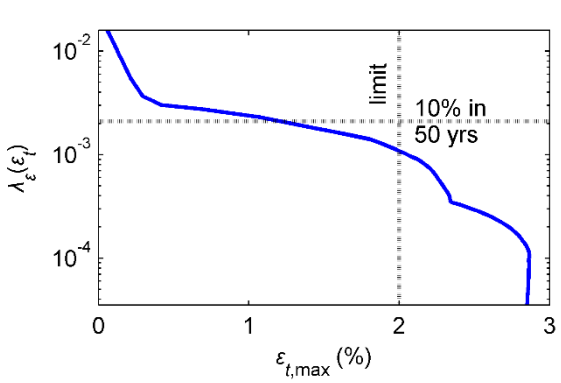

Figure 4: Results from every step of the proposed methodology for the reference pipeline.

Structural analysis results are used in the deterministic evaluation of the effectiveness of protection measures, where neither fault offset randomness, nor demand and capacity uncertainties are considered. Then, strain demand is compared to strain capacity (code-based strain limits) for a single fault offset magnitude, usually the maximum or the characteristic. However, this is only a point estimate of the failure potential and depending on the adopted scenario assumptions it may result either in overconservative and uneconomical design or, sometimes, in unsafe one. Therefore, strain hazard analysis (third step) is necessary to achieve a balance between safety and economy.

The examined measures have been evaluated in a deterministic manner in [7], where it was concluded that trench backfilling with pumice (P), use of culverts (C) and use of flexible joints (PFJ) are efficient ones, while steel grade upgrade (S) and wall thickness increase (W) are not. In order then to acquire qualitative and quantitative understanding on the differences between the usually adopted deterministic approach and the probabilistic one, the aforementioned distinction is adopted hereinafter. Therefore, results are presented firstly for cases P, C and PFJ (Measures of group 1 – section 5.1) in comparison to the reference pipe (R) and secondly for cases S and W (Measures of group 2 – section 5.2). For comparison reasons, results from steps 2 and 3 of the methodology are presented together for every pipe – fault crossing angle and separately for tensile and compressive strains.

5.1 Measures of group 1

The evolution of tensile and compressive strains with respect to the normalized fault offset are depicted in Figure 5(a) and Figure 6(a), respectively, for pipe – fault crossing angle

$\beta = 75^{o}$. All measures are shown to be effective in terms of reducing developing pipe strains, besides PFJ in tension for very high fault offset. The corresponding hazard curves for tensile and compressive strains are depicted in Figure 5(b) and Figure 6(b), respectively. It is indicated from tensile strain hazard curves in Figure 5(b) that the reference pipeline (R) has MAR of exceeding tensile limit strain equal to 9.32×10^{-4} and the pipe with flexible joints (PFJ) equal to 0.72×10^{-4}, while the corresponding MARs for pumice backfilling (P) and culverts (C) cases are approximately equal to zero. The reference pipe might fail due to tensile rupture with MAR about three times lower than the 10% probability in 50 years, while the failure of the pipe with joints is about 12 times less frequent. At the same time, pumice backfilling and use of culverts are shown to be significantly effective measures as the potential of tensile failure is very low. Evaluating the compressive strain hazard curves shown in Figure 6(b), one can identify that local buckling is not expected to occur, given that pipes are subjected mainly to tension resulting from the geometry of pipe – fault crossing, i.e. angle $\beta = 75^{o}$. As an additional remark for compressive strains, for low fault offset the pipe is subjected mainly to bending and consequently tension and compression increase progressively. Then, for higher fault offset, the pipe is mainly elongated and thus compression decreases, thus the peculiar shape of Figure 6(a),(b). In such “re-entrant” strain hazard curves, as shown in Figure 6(b), one should take care to always report the higher value of λ_{LS} where multiple values may correspond to a single strain capacity, as would be the case for example for a capacity of 0.2%.

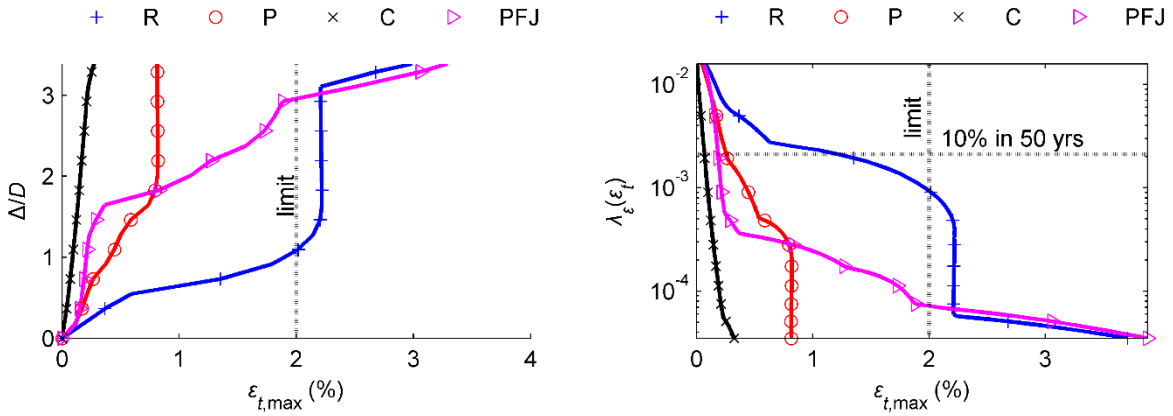

(a) (b)

Figure 5: (a) Maximum tensile strain ($\varepsilon_{t,max}$) with respect to normalized fault displacement (Δ/D) and (b) tensile strain hazard curve for crossing angle β = 75° (R: reference pipe, P: pumice backfill, C: use of culverts and PFJ: use of flexible joints)

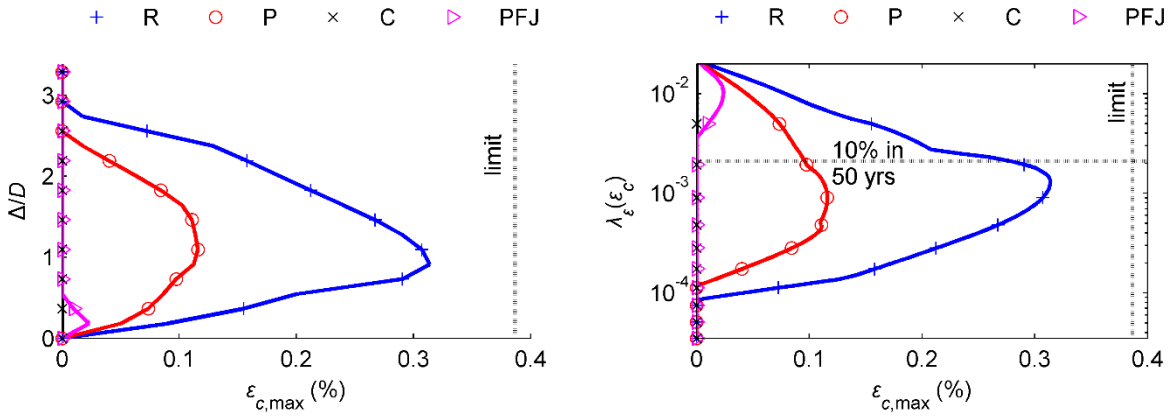

(a) (b)

Figure 6: (a) Maximum compressive strain ($\varepsilon_{t,max}$) with respect to normalized fault displacement (Δ/D) and (b) compressive strain hazard curve for crossing angle β = 75° (R: reference pipe, P: pumice backfill, C: use of culverts and PFJ: use of flexible joints)

Perpendicular pipe – fault crossing (β = 90°) is recommended by structural codes, for example, in Eurocode 8 – Part 4 [22], in order to avoid significant tension or compression. The maximum tensile and compressive strains relative to the fault offset are depicted in Figure 7(a) and Figure 8(a), respectively, where it is observed that measures P, C and PFJ are all effective in preventing both tensile rupture and local buckling. These findings are

verified by the corresponding strain hazard curves of Figure 7(b) and Figure 8(b). The MAR of exceeding tensile strain limit state for the reference pipe is $\lambda_{LS,t}$ = 10.85×10^{-4}, which is about 2.5 times lower than λ = 21×10^{-4}, while the MAR of exceeding compressive limit state is $\lambda_{LS,c}$ = 29.59×10^{-4}, which is higher than λ = 21×10^{-4}, indicating the potential of local buckling being more frequent than 10% in 50 years. It is notable that the compressive demand of the unprotected reference pipe can be seen as “infinite”, in the sense that local buckling is expected to occur for relatively very low fault offset and therefore $\varepsilon_{c,dem}$ = ∞, or a very high value for numerical purposes.

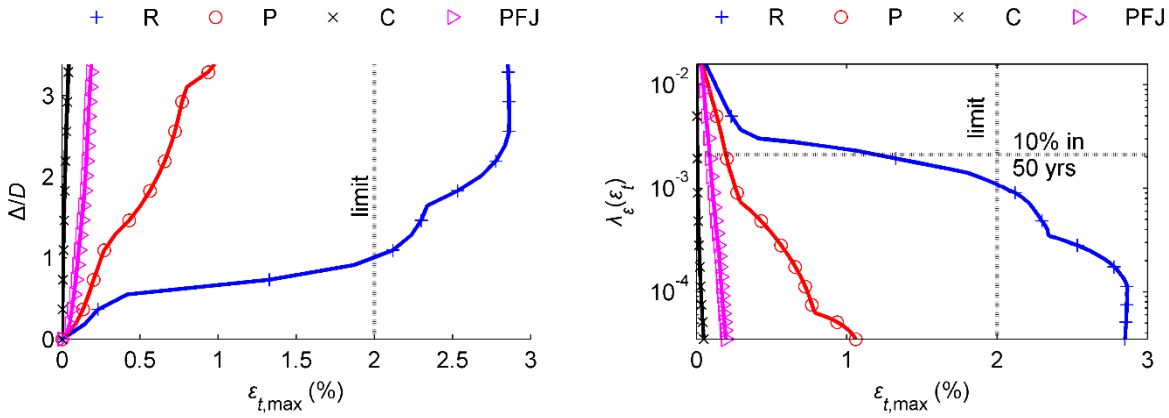

(a) (b)

Figure 7: (a) Maximum tensile strain ($\varepsilon_{t,max}$) with respect to normalized fault displacement (Δ/D) and (b) tensile strain hazard curve for crossing angle β = 90^o (R: reference pipe, P: pumice backfill, C: use of culverts and PFJ: use of flexible joints)

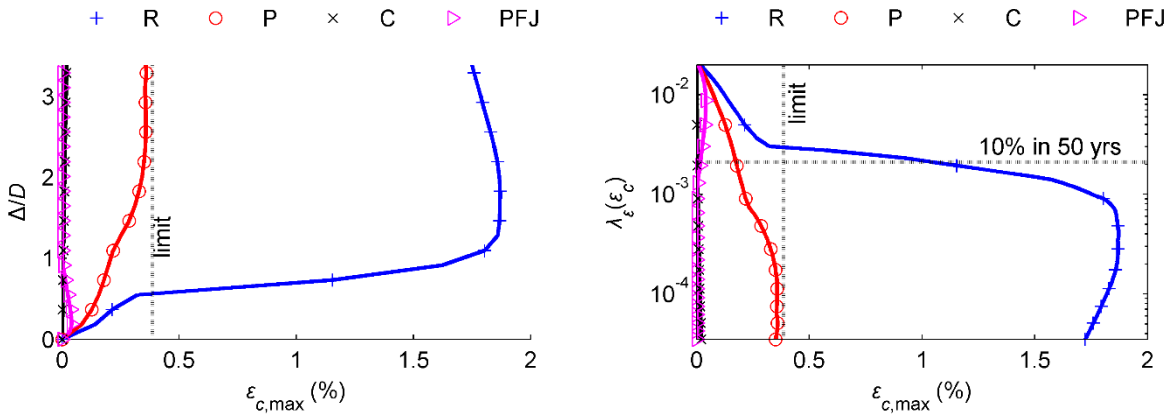

(a) (b)

Figure 8: (a) Maximum compressive strain ($\varepsilon_{t,\max}$) with respect to normalized fault displacement (Δ/D) and (b) compressive strain hazard curve for crossing angle $\beta = 90^{o}$ (R: reference pipe, P: pumice backfill, C: use of culverts and PFJ: use of flexible joints)

5.2 Measures of group 2

Strengthening protection measures, namely steel upgrade (S) and wall thickness increase (W) have been found in [7] to be quite ineffective in protecting the pipe against failure due to faulting. However, it is essential to re-examine these measures on a performance basis in order to extract the corresponding rates of failure, rather than examining the efficiency based on a single level of fault offset.

In case the pipe – fault crossing angle equals $\beta = 75^{o}$, the maximum tensile and compressive strains with respect to the fault offset are shown in Figure 9(a) and Figure 10(a), respectively. It is detected that indeed the contribution of measures S and W to pipe protection in terms of strain reduction is not significant. The corresponding strain hazard curves are displayed in Figure 9(b) and Figure 10(b), respectively. The MARs of exceeding tensile strain limit state are: for the reference pipe $\lambda_{LS,t} = 9.32\times10^{-4}$, steel grade upgrade $\lambda_{LS,t} \approx 0$ and wall thickness increase $\lambda_{LS,t} \approx 0$. Therefore, the failure rates of measures S and W indicate that adequate protection can be provided. The same outcomes are derived from the compression strain hazard curves shown in Figure 10(b).

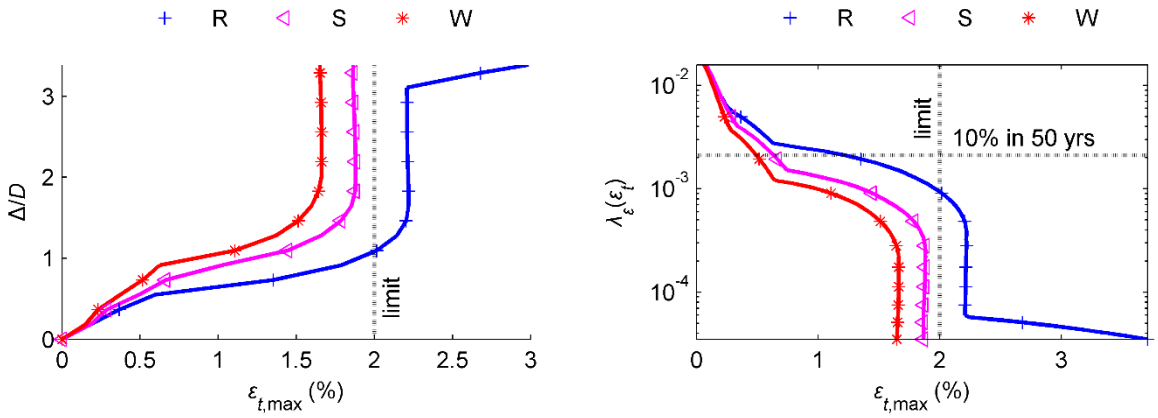

(a) (b)

Figure 9: (a) Maximum tensile strain ($\varepsilon_{t,\max}$) with respect to normalized fault displacement (Δ/D) and (b) tensile strain hazard curve for crossing angle $\beta = 75^{o}$ (R: reference pipe, S: steel grade upgrade and W: wall thickness increase)

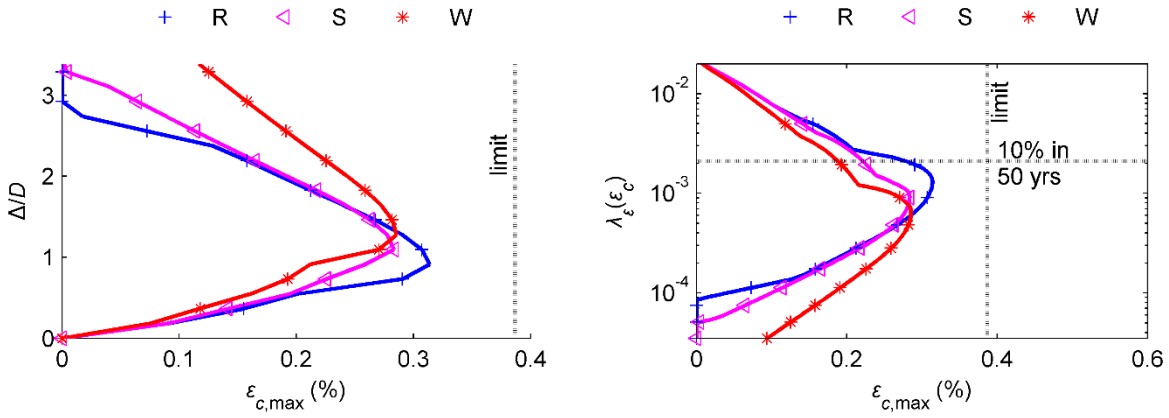

(a) (b)

Figure 10: (a) Maximum compressive strain ($\varepsilon_{t,\max}$) with respect to normalized fault displacement (Δ/D) and (b) compressive strain hazard curve for crossing angle $\beta = 75^{o}$ (R: reference pipe, S: steel grade upgrade and W: wall thickness increase)

Finally, in case the pipe – fault crossing equals $\beta = 90^{o}$, structural analysis results are illustrated in Figure 11(a) and Figure 12(a). It is demonstrated that none of the measures in question (S and W) can provide sufficient tensile or compressive strain reduction and therefore pipe failure can occur for relatively low fault offsets. In such cases, it is crucial to find the rate of failure occurrence. The tensile and compressive strain hazard curves are depicted in Figure 11(b) and Figure 12(b), respectively. The MARs of exceeding tensile strain limit are: for reference pipe $\lambda_{LS,t} = 10.85\times10^{-4}$, for steel upgrade $\lambda_{LS,t} = 3.61\times10^{-4}$ and for wall thickness increase $\lambda_{LS,t} = 0.99\times10^{-4}$. These rates indicate that pipe strengthening measures can be considered under specific conditions as effective against tensile rupture for the case under investigation. In particular, the failure rate for steel upgrade is about three times lower than the one for the reference pipe and the corresponding one for wall thickness increase is about 10 times lower. Then, the MARs of exceeding the compressive strain limit are: for reference pipe $\lambda_{LS,c} = 29.57\times10^{-4}$, for steel upgrade $\lambda_{LS,c} = 17.31\times10^{-4}$ and for wall

thickness increase $\lambda_{LS,t}$ = 14.77×10^{-4}. In case measures S and W are used, occurrence of local buckling is less frequent by roughly one half compared to the reference pipe. The MARs of exceeding tensile and compressive strain limit states are summarized in Table 3 and Table 4 for crossing angles β = 75^{o} and β = 90^{o}, respectively.

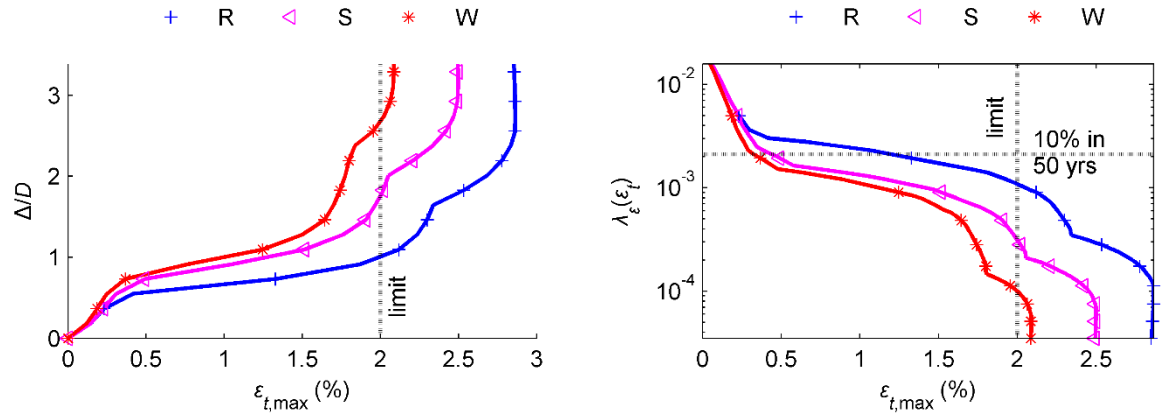

(a) (b)

Figure 11: (a) Maximum tensile strain ($\varepsilon_{t,max}$) with respect to normalized fault displacement (Δ/D) and (b) tensile strain hazard curve for crossing angle β = 90^{o} (R: reference pipe, S: steel grade upgrade and W: wall thickness increase)

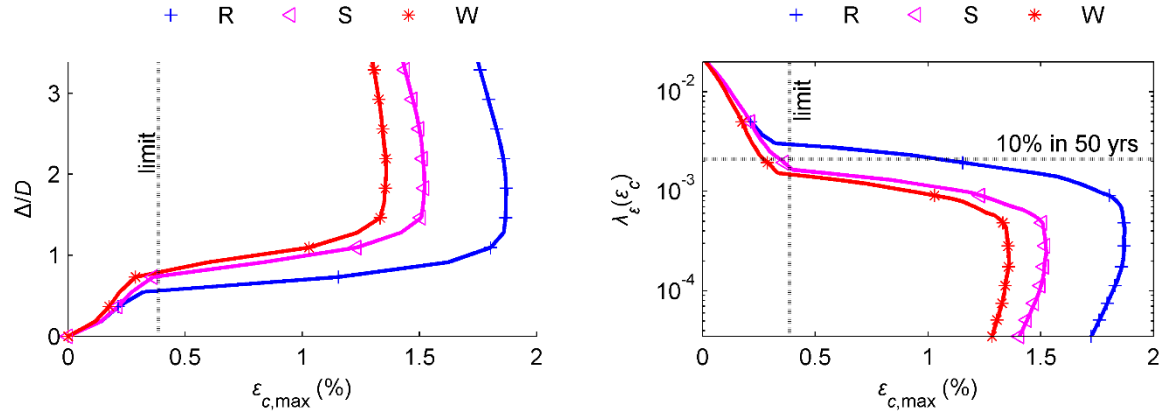

(a) (b)

Figure 12: (a) Maximum compressive strain ($\varepsilon_{t,max}$) with respect to normalized fault displacement (Δ/D) and (b) compressive strain hazard curve for crossing angle β = 90^{o} (R: reference pipe, S: steel grade upgrade and W: wall thickness increase)

Table 3: Mean annual rate of exceeding tensile rupture and local buckling limit states for pipe – fault crossing angle $\beta = 75^{o}$.

Case	Protection measure	$\lambda_{LS,t}$	$\lambda_{LS,c}$
R	(reference pipe)	9.32×10^{-4}	~0
P	trench backfilling with pumice	~0	~0
C	use of culverts	~0	~0
PFJ	use of flexible joints	0.72×10^{-4}	~0
S	steel grade upgrade	~0	~0
W	wall thickness increase	~0	~0

Table 4: Mean annual rate of exceeding tensile rupture and local buckling limit states for pipe – fault crossing angle $\beta = 90^{o}$.

Case	Protection measure	$\lambda_{LS,t}$	$\lambda_{LS,c}$
R	(reference pipe)	10.85×10^{-4}	29.57×10^{-4}
P	trench backfilling with pumice	~0	~0
C	use of culverts	~0	~0
PFJ	use of flexible joints	~0	~0
S	steel grade upgrade	3.61×10^{-4}	17.31×10^{-4}
W	wall thickness increase	0.99×10^{-4}	14.77×10^{-4}

Demand (given the mean hazard) and capacity uncertainties are not considered in the strain hazard curves presented earlier. Thus, the corresponding MARs of exceeding failure limit states that are listed in Table 3 and Table 4 may be easily obtained as the intersection ordinate of the strain hazard curve and the capacity limit. According to the aforementioned discussion (section 2.4), demand and capacity uncertainties are inherent to the problem and assuming typical values of such uncertainties with $\beta_{uD} = 0.35$ and $\beta_{uC} = 0.35$, Eq. (14) yields an overall uncertainty of $\beta_u = 0.50$. Then, adopting an $x = 95\%$ confidence level, the safety margin after Eq. (13) equals $SM = 2.26$. The capacity-to-demand ratio (CDR) for 10% probability of exceedance in 50 years is the ratio of the strain capacity (2% tensile strain and 0.39% compressive strain) over the strain demand, which is the intersection abscissa of the strain hazard curve and the 10% in 50 yrs horizontal line.

Then, CDRs are calculated for every examined case, separately for tension (CDR_t) and compression (CDR_c), and are listed in Table 5 and Table 6 for crossing angles $\beta = 75^o$ and $\beta = 90^o$, respectively. Safety checking is performed by comparing *CDR* to *SM* = 2.26. In case *CDR* < *SM*, then the safety requirement is not met at the 95% confidence level and the corresponding values are shown in brackets. Furthermore, *SM* values provide qualitative and quantitative information on the effectiveness of measures in terms that the engineer is able to decide whether the available safety margin is acceptable or not and whether it complies with the requirements of the customer. Finally, results from cases of steel grade upgrade (S) and wall thickness increase (W) indicatively for crossing angle $\beta = 90^o$ highlight also the importance of uncertainties. The failure rates for compression are $\lambda_{LS,c} = 17.31 \times 10^{-4}$ and $\lambda_{LS,c} = 14.77 \times 10^{-4}$ (Table 4), respectively, which are lower than $\lambda = 0.0021$ indicating safe design. As expected, however, considering demand and capacity uncertainties, the corresponding CDRs in Table 6 are 1.14 and 1.44 that are lower than *SM* = 2.52, indicating unsafe designs or inadequate safety, given the assumptions of the analysis.

Table 5: Capacity-to-demand ratio for tensile strains and 10% probability of exceedance in 50 years for pipe – fault crossing angle $\beta = 75^o$ (failure is indicated in brackets).

Case	Protection measure	CDR_t	CDR_c
R	(reference pipe)	[1.63]	[1.40]
P	trench backfilling with pumice	7.83	4.07
C	use of culverts	29.85	+∞
PFJ	use of flexible joints	10.84	+∞
S	steel grade upgrade	3.15	[2.08]
W	wall thickness increase	4.06	[1.76]

Table 6: Capacity-to-demand ratio for tensile strains and 10% probability of exceedance in 50 years for pipe – fault crossing angle $\beta = 90^o$ (failure is indicated in brackets).

Case	Protection measure	CDR_t	CDR_c
R	(reference pipe)	[1.66]	[0.37]
P	trench backfilling with pumice	10.19	[2.23]
C	use of culverts	+∞	+∞

PFJ	use of flexible joints	23.26	22.95
S	steel grade upgrade	4.51	[1.14]
W	wall thickness increase	[0.99]	[1.44]

6. SUMMARY AND CONCLUSIONS

A three-step methodology for performance-based assessment of protection measures for buried pipelines at fault crossings has been presented. The first step consists of seismic hazard analysis, adjusting the Probabilistic Fault Displacement Hazard Analysis for pipe – fault crossing and considering the pertinent epistemic uncertainties through a logic tree formulation and the aleatory uncertainties through sampling. The second step includes the assessment of pipe mechanical behavior by implementing nonlinear numerical analysis using beam-type finite element models. Finally, seismic hazard and structural analysis results are combined to estimate the hazard through the strain hazard curves (third step), which are easy-to-handle engineering decision making tools.

The above approach has been cast within a safety factor format for practical decision-making under uncertainty. The application to a simple case study of a pipeline – strike-slip fault crossing showed the difference between a deterministic approach and probabilistic approaches with and without uncertainties incorporated. Five different protection measures are thus evaluated, showing how one can draw very different conclusions on the safety of each protection method, based on the approach taken and the pertinent assumptions on the magnitude of uncertainties. All in all, it is argued that an uncertainty conscious probabilistic approach is best suited to provide the necessary safety, not because of different or more accurate structural analysis but because of more consistently handling the different scenarios in an uncertain setting.

ACKNOWLEDGMENTS

This research has been co-financed by the European Union (European Social Fund – ESF) and Hellenic National Funds through the Operational Program “Education and Lifelong Learning” (NSRF 2007-2013) – Research Funding Program “Aristeia II”, project

“ENSSTRAM - Novel Design Concepts for Energy Related Steel Structures using Advanced Materials”, grant number 4916 and the European Social Funds through the Operational Program “Human Resources Development” of the National Strategic Framework (NSRF) 2007-2013, project “Direct Methodology for Performance Based Seismic Design”.

REFERENCES

[1] O’Rourke MJ, Liu X. Seismic design of buried and offshore pipelines. Monograph No. 4”. Buffalo: Multidisciplinary Center for Earthquake Engineering Research; 2012.

[2] Melissianos VE, Vamvatsikos D, Gantes CJ. Performance assessment of buried pipelines at fault crossings. Earthquake Spectra 2017;33(1):201-218. doi: 10.1193/122015EQS187M

[3] Cornell CA, Krawinkler H. Progress and Challenges in Seismic Performance Assessment. PEER Center News 2000;3(2):1–4.

[4] Youngs RR, Arabasz WJ, et al. A methodology for probabilistic fault displacement hazard analysis (PFDHA). Earthquake Spectra 2003;19(1):191–219. doi: 10.1193/1.1542891

[5] Cornell CA, Jalayer F, Hamburger RO, Foutch DA. Probabilistic basis for 2000 SAC Federal Emergency Management Agency steel moment frame guidelines. ASCE J Struct Eng 2002;128(4):526–533. doi: 10.1061/(ASCE)0733-9445(2002)128:4(526)

[6] ALA American Lifelines Alliance. Guideline for the design of buried steel pipe – July 2001 (with addenda through February 2005). American Society of Civil Engineers, New York, USA; 2005.

[7] Gantes CJ, Melissianos VE. Evaluation of seismic protection methods for buried fuel pipelines subjected to fault rupture. Frontiers in Built Environment 2016;2:34. doi:10.3389/fbuil.2016.00034

[8] Cornell CA. Engineering seismic risk analysis. Bulletin of the Seismological Society of America 1968;58(5):1583–1606.

[9] Petersen MD, Dawson, TE, et al. Fault displacement hazard for strike-slip fault. Bulleting of the Seismological Society of America 2011;110(2):805-825. doi: 10.1785/0120100035

[10] Wells DL, Coppersmith KJ. New empirical relationships among magnitude, rupture length, rupture width, rupture area, and surface displacement. Bulletin of the Seismological Society of America 1994;84(4):974–1002.

[11] Gutenberg B, Richter CF. Frequency of earthquakes in California. Bulletin of the Seismological Society of America 1944;34(4):185.

[12] Kramer SL. Geotechnical earthquake engineering: Prentice-Hall; 1996.

[13] Chen Y, Akkar S. Probabilistic permanent fault displacement hazard via Monte Carlo simulation and its consideration for the probabilistic risk assessment of buried continuous steel pipelines. Earth Eng Struct Dyn 2017;46(4):605-620. doi: 10.1002/eqe.2805

[14] Bommer JJ, Scherbaum F. The use and misuse of logic trees in probabilistic seismic hazard analysis. Earthquake Spectra 2008;24(4):997–1009. doi: 10.1193/1.2977755

[15] Abrahamson NA, Bommer JJ. Probability and uncertainty in seismic hazard analysis. Earthquake Spectra 2005;21(2):603–607. doi: 10.1193/1.1899158

[16] Joshi S, Prashant A, Deb A, Jain SK. Analysis of buried pipelines subjected to reverse fault motion. Soil Dyn Earthq Eng 2011;31:930-40. DOI: 10.1016/j.soildyn.2011.02.003

[17] Uckan E, Akbas B, Shen J, Rou W, Paolacci F, O'Rourke M. A simplified analysis model for determining the seismic response of buried steel pipes at strike-slip fault crossings. Soil Dyn Earthq Eng 2015;75:55-65. doi: 10.1016/j.soildyn.2015.03.001

[18] Liu X, Zhang H, Han Y, Xia M, Zheng W. A semi-empirical model for peak strain prediction of buried X80 steel pipelines under compression and bending at strike-slip fault crossings. J Nat Gas Sci Eng 2016;32:465-475. doi: 10.1016/j.jngse.2016.04.054.

[19] Rahman MA, Taniyama H. Analysis of a buried pipeline subjected to fault displacement: A DEM and FEM study. Soil Dyn Earthq Eng 2015:71;49–62. doi: 10.1016/j.soildyn.2015.01.011

[20] Trifonov OV. Numerical stress-strain analysis of buried steel pipelines crossing active strike-slip faults with an emphasis on fault modeling aspects. ASCE J Pipeline Syst Eng Pract 2015;6(1):04014008. doi: 10.1061/(ASCE)PS.1949-1204.0000177

[21] Vazouras P, Dakoulas P, Karamanos SA. Pipe-soil interaction and pipeline performance under strike-slip fault movements. Soil Dyn Earthq Eng 2015;72:48-65. DOI: 10.1016/j.soildyn.2015.01.014

[22] Comité Européen de Normalisation. Eurocode 8, Part 4: Silos, tanks and pipelines. CEN EN 1998-4, Brussels, Belgium; 2006.

[23] Tesfamariam S, Goda K. Handbook of seismic risk analysis and management of civil infrastructure systems: Woodhead Publishing Limited;2013.

[24] Federal Emergency Management Agency. FEMA 350. Recommended seismic design criteria for new steel moment frame buildings: Washington, DC;2000.

[25] Comité Européen de Normalisation. Eurocode 0 Basis of structural design. CEN EN 1990, Brussels, Belgium; 2005.

[26] Gantes CJ, Bouckovalas GD. Seismic verification of high pressure natural gas pipeline Komotini – Alexandropoulis – Kipi in areas of active fault crossings. Struct Eng Int 2013;2:204-8. doi: 10.2749/101686613X13439149157164

[27] Melissianos VE, Korakitis GP, Gantes CJ, Bouckovalas GD. Numerical evaluation of the effectiveness of flexible joints in buried pipelines subjected to strike-slip fault rupture. Soil Dyn Earthq Eng 2016;90:395-410. doi: 10.1016/j.soildyn.2016.09.012

[28] Melissianos VE, Lignos XA, Bachas KK, Gantes CJ. Experimental investigation of pipes with flexible joints under fault rupture. J Const Steel Res 2017;128:633-648. doi: 10.1016/j.jcsr.2016.09.026

[29] Karamanos SA, Keil B, Card RJ. Seismic design of buried steel water pipelines, In: Proceedings of the Pipelines 2014: From Underground to the Forefront of Innovation and Sustainability; 2015 Aug 3-6; Portland, Oregon, USA, p. 1005-19. doi: 10.1061/9780784413692.091

[30] Fragiadakis M, Vamvatsikos, Karlaftis MG, Lagaros ND, Papadrakakis M. Seismic assessment of structures and lifelines. J Sound Vib 2015;334:29-56. doi: 10.1016/j.jsv.2013.12.031

[31] Akkar S, Sandıkkaya MA, Şenyurt M, et al. Reference database for seismic ground-motion in Europe (RESORCE). Bull Earthquake Eng 2014;12(1):311-339. doi:10.1007/s10518-013-9506-8

[32] Woessner J, Laurentiu D, Giardini D, et al. The 2013 European Seismic Hazard Model: key components and results. Bull Earthquake Eng 2015;13(12):3553-96. doi:10.1007/s10518-015-9795-1

[33] ADINA R & D Inc. Theory and Modeling guide Volume I: ADINA, Report AED 06-7, Watertown, USA; 2006.

[34] Melissianos VE, Gantes CJ. Numerical modeling aspects of buried pipeline – fault crossing. In: Papadrakakis M, Plevris V, Lagaros ND, editors. Computational Methods in Earthquake Engineering Volume 3, Computational Methods in Applied Sciences series. Berlin: Springer Verlag; 2016. p 1-26. doi: 10.1007/978-3-319-47798-5_1

[35] Kojic M, Bathe KJ. Inelastic analysis of solid and structures, Computational Fluid and Solid Mechanics series, Berlin: Springer Verlag; 2004.

[36] Peng LC, Peng A. Pipe stress engineering, New York: ASME Press; 2009.

[37] EJMA. Standards of the expansion joint manufacturers association, inc. 9th ed. Tarrytown, New York, USA: Expansion Joints Manufacturers Association, Inc.; 2008.